

Cycloaddition of Biomass-Derived Furans for Catalytic Production of Renewable *p*-Xylene

C. Luke Williams,[†] Chun-Chih Chang,[†] Phuong Do,[‡] Nima Nikbin,[‡] Stavros Caratzoulas,[‡] Dionisios G. Vlachos,[‡] Raul F. Lobo,[‡] Wei Fan,[†] and Paul J. Dauenhauer^{†,*}

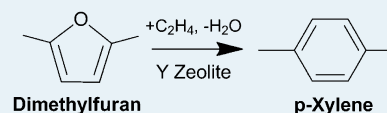
[†]Department of Chemical Engineering and Catalysis Center for Energy Innovation, University of Massachusetts, 686 North Pleasant Street, Amherst, Massachusetts 01003, United States

[‡]Department of Chemical Engineering and Catalysis Center for Energy Innovation, University of Delaware, 150 Academy Street, Newark, Delaware 19716, United States

Supporting Information

ABSTRACT: A renewable route to *p*-xylene from biomass-derived dimethylfuran and ethylene is investigated with zeolite catalysts. Cycloaddition of ethylene and 2,5-dimethylfuran and subsequent dehydration to *p*-xylene has been achieved with 75% selectivity using H–Y zeolite and an aliphatic solvent at 300 °C. Competitive side reactions include hydrolysis of dimethylfuran to 2,5-hexanedione, alkylation of *p*-xylene, and polymerization of 2,5-hexanedione. The observed reaction rates and computed energy barriers are consistent with a two-step reaction that proceeds through a bicyclic adduct prior to dehydration to *p*-xylene. Cycloaddition of ethylene and dimethylfuran occurs without a catalytic active site, but the reaction is promoted by confinement within microporous materials. The presence of Brønsted acid sites catalyzes dehydration of the Diels–Alder cycloadduct (to produce *p*-xylene and water), and this ultimately causes the rate-determining step to be the initial cycloaddition.

KEYWORDS: xylene, furan, Diels–Alder, zeolite, ethylene

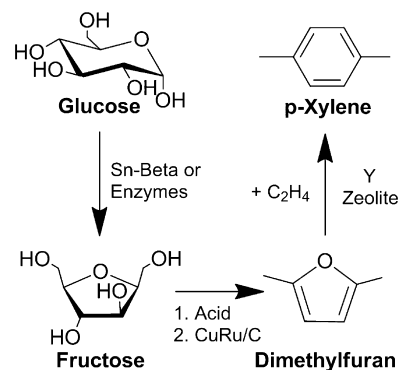


Increasing demand for energy and materials has led to an accelerated research effort in the development of renewable chemicals for a sustainable economy.¹ Cellulose and hemicellulose make up as much as 70 wt % of lignocellulosic biomass and consist of five- (e.g., xylose) and six-carbon sugars (glucose).² These sugars, obtained by saccharification of biopolymers (e.g., cellulose, hemicellulose), are considered the primary feedstocks for renewable chemical processes.³

One important chemical, *p*-xylene, is used for the production of terephthalic acid,⁴ a monomer for polyester and polyethylene terephthalate plastics (e.g., plastic bottles).⁵ *p*-Xylene is currently produced from the separation of aromatic mixtures (isomers of xylene and ethylbenzene) from the naptha fraction of petroleum. *p*-Xylene can also be selectively produced from toluene through the use of ZSM-5 catalysts^{6,7} in combination with membrane separation.^{7,8} New processes are currently being implemented to produce *p*-xylene from renewable resources using a hybrid process that combines fermentation and heterogeneous catalysis.^{9–12}

p-Xylene can potentially be produced renewably starting from glucose, as shown in Scheme 1. Isomerization of glucose to fructose can be performed using biological (i.e., enzymes) or thermochemical catalysts including base catalysts¹³ or Lewis acid heterogeneous catalysts such as Sn-Beta.¹⁴ Fructose can then be converted to hydroxymethylfurfural,¹⁵ which can be hydrodeoxygenated to produce dimethylfuran¹⁶ in an overall process designed to produce biofuels. To produce *p*-xylene, dimethylfuran must then be converted in two-steps: Diels–Alder cycloaddition of ethylene followed by dehydration.¹⁷

Scheme 1. Renewable Process for Production of *p*-Xylene from Glucose



In this scheme, the conversion of dimethylfuran to *p*-xylene by a two-step reaction (cycloaddition followed by dehydration) is crucial for the efficient production of high-value chemicals from biomass-derived sugars; however, the precise chemical mechanism producing *p*-xylene and side products as well as heterogeneous catalysts that easily integrate the selective conversion of dimethylfuran to *p*-xylene is lacking. The initial step in the conversion of dimethylfuran to *p*-xylene is thought to occur by the Diels–Alder reaction¹⁸ with ethylene as the

Received: January 7, 2012

Revised: April 1, 2012

Published: April 18, 2012

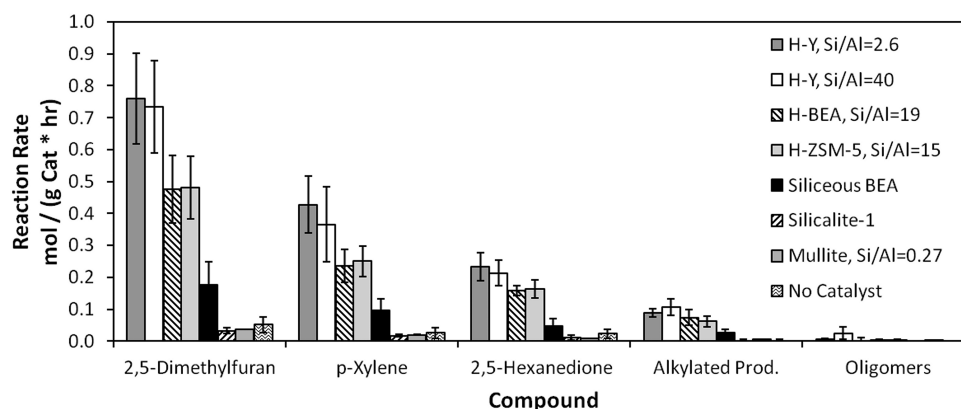


Figure 1. Initial catalytic reaction rates of dimethylfuran cycloaddition with ethylene. The initial reaction rate of dimethylfuran conversion ($X_{\text{DMF}} < 10\%$) and product formation vary for catalyst microstructure and active site. Reaction rates were measured using pure dimethylfuran with the continuous addition of C_2H_4 (57 bar) at 300 °C. Error bars represent a 90% confidence interval.

dienophile. It is known that furans undergo [4 + 2]-cycloaddition with a number of dienophiles, including alkynes and alkenes, but the reaction environment and functionality of the diene/dienophile leads to significant variation in activity and stereochemistry.¹⁹

Employing ethylene as the dienophile in Diels–Alder processes is inherently difficult; ethylene lacks an electron-withdrawing group that promotes the reaction by closing the HOMO–LUMO gap of the interacting molecules. For a large number of substituted furans, [4 + 2]-cycloaddition with an alkene results in the formation of an oxabicyclic cycloadduct.^{20,21} This step has been catalyzed by a number of Lewis acids, including ZnCl_2 ,²² ZnI_2 ,²² and Et_2AlCl .²³ Similarly, cycloaddition of other dienes/dienophiles has been catalyzed by zeolites such as Y, beta and ZSM-5,²⁴ some of which were exchanged with cations such as sodium²⁵ or copper.²⁶

We investigate here the catalytic conversion of dimethylfuran to *p*-xylene and demonstrate high yield using zeolite Y catalysts. By reacting liquid dimethylfuran with high-pressure ethylene, we identify (and attempt to minimize through catalyst design) competitive side reactions that reduce *p*-xylene yield. In addition, we find that Diels–Alder cycloaddition (the first step in conversion of DMF to *p*-xylene) does not utilize an active site but is promoted primarily by confinement within zeolites. The second step (dehydration) is catalyzed by Brønsted acid sites, rendering the first reaction step (cycloaddition) rate-determining.

■ CATALYST PREPARATION/CHARACTERIZATION

The proton forms of H–Y, H-Beta, and H-ZSM-5 catalysts were provided by Zeolyst and calcined at 550 °C prior to use in reaction testing. H–silica–alumina was prepared by heating silica–alumina (catalyst support grade 135, Aldrich) at 500 °C for 16 h. Mullite (crystalline aluminum silicate; Si/Al = 0.27, Aldrich) was calcined at 550 °C for 12 h before use in reaction tests. Siliceous beta and silicalite-1 were prepared using established protocols.^{27–29} The number of Brønsted acid sites was characterized by temperature-programmed desorption coupled with thermo-gravimetric analysis (TPD–TGA) for isopropylamine,³⁰ whereas total acid sites was determined by using ammonia temperature-programmed desorption (NH_3 -TPD). Catalyst surface area was determined using N_2 sorption isotherms, and crystal structures and morphologies of the catalysts were determined by X-ray powder diffraction (X'Pert

PRO diffractometer (PANalytical)) and scanning electron microscopy (Magellan 400 (FEI)). Additional details of both catalyst preparation and characterization are given in the Supporting Information.

■ EXPERIMENTAL SETUP

Reactions were carried out in a 100 mL, high-pressure, high-temperature Parr benchtop reactor (model 4598HTHP with a 4848 temperature controller) using both commercially available and in-house synthesized zeolite catalysts. 2,5-Dimethylfuran (99.5+% Alfa Aesar and 99.5+% Acros Organics) was reacted with zeolite catalysts over a temperature range of 200 to 300 °C with a loading of 0.25 g of catalyst to 49 mL of reactant and 1 mL of *n*-tridecane as an internal standard (98+% Sigma). The reaction vessel was purged with N_2 and stirred at 1000 rpm with a gas entrainment impeller while heating to the reaction conditions. Once the reaction temperature was achieved, the vessel was pressurized to 57 bar (825 psi) with ethylene gas, which was continuously added during the reaction. Samples were collected immediately after ethylene addition and at later times corresponding to a dimethylfuran conversion of about 10% while the system was at reaction conditions. Products were identified using a gas chromatograph/mass spectrometer and by comparing retention times with those of pure standards. Quantification was performed using a gas chromatograph equipped with a flame ionization detector. Further details about the reactor, sampling procedure, and analysis are provided in the Supporting Information.

■ CALCULATION

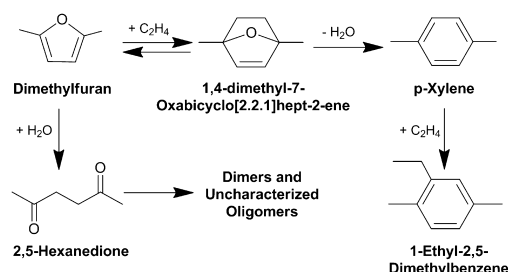
All computed thermochemistry and reaction pathway data reported herein are based on gas-phase electronic structure calculations; they were performed with Gaussian 09³¹ at the DFT-M062X theory level with the 6-311+G(d,p) basis set. The transition structures correspond to first-order saddle points in the potential energy hypersurface and were verified by frequency (i.e., presence of a single imaginary frequency) as well as internal reaction coordinate calculations. The Gibbs thermal energies do not include frequency rescaling. The Brønsted acid-catalyzed dehydration reaction of the Diels–Alder cycloadduct was modeled by protonation of the cycloadduct.

RESULTS AND DISCUSSION

Experimental examination of the catalytic cycloaddition of ethylene and dimethylfuran shows that the reaction occurs within a four-phase system free of transport limitations (see below). Ethylene gas is absorbed within liquid dimethylfuran containing solid catalyst. A fourth phase, liquid water, was observed to form as the reaction proceeds. Mass transfer experiments indicate an ethylene mass transfer rate of $k_L a = 6.16 \text{ h}^{-1}$ within dimethylfuran resulting from a gas-entrainment impeller (Supporting Information, Figure S6). For an H–Y catalyst at $300 \text{ }^\circ\text{C}$, the reaction rate constant (k_{rxn}) is 0.166 h^{-1} (Supporting Information, Figure S6). Combined with the mass transfer coefficient ($k_L a$), this rate constant gives a Damköhler number ($\text{Da} = k_{\text{rxn}}/k_L a$) of 0.027, which indicates that ethylene is transferred into the liquid faster than it reacts. In addition, the calculated Weisz–Prater criterion for this system is 0.039, indicating the absence of intraparticle transport limitations (Supporting Information, Table S7).

Initial reaction rates for the cycloaddition and dehydration of dimethylfuran and ethylene were measured for multiple catalysts at low conversion ($X_{\text{DMF-Average}} = 8.9 \pm 1.5\%$) at $300 \text{ }^\circ\text{C}$, as shown in Figure 1. The reaction of dimethylfuran and ethylene without a catalyst exhibited a slow reaction rate and resulted in a low conversion ($X_{\text{DMF}} < 8.5\%$ after 25 h of reaction time). The noncatalytic system exhibited the same reaction rates as silicalite-1 ($0.03 \text{ mol g}_{\text{cat}}^{-1} \text{ hr}^{-1}$) and mullite (nonporous crystalline aluminum silicate without acid sites) ($0.04 \text{ mol g}_{\text{cat}}^{-1} \text{ hr}^{-1}$). The addition of Brønsted acid sites in H-BEA (0.56 mmol/g) and H-ZSM-5 (0.71 mmol/g) increased the reaction rates ($0.48 \pm 0.1 \text{ mol g}_{\text{cat}}^{-1} \text{ hr}^{-1}$) for both catalysts, which is about an order of magnitude increase over the rate of their siliceous counterparts. Further improvement in catalyst activity was observed with H–Y catalyst, which exhibited a higher reaction rate of about $0.74 \text{ mol g}_{\text{cat}}^{-1} \text{ hr}^{-1}$ independent of the Si/Al ratio. H–Y catalysts with Si/Al ratios of 2.6, 30, and 40 exhibited catalytic performance that was not statistically different. H–Y catalyst (Si/Al = 30) was regenerated for three consecutive trials with no statistically significant loss in activity (Supporting Information, Figure S4). In comparison, an amorphous silica–alumina catalyst with Brønsted acid sites (0.34 mmol/g) was more active than H–Y catalyst but exhibited almost no selectivity to *p*-xylene, <5%. Similar selectivity to major products, *p*-xylene and 2,5-hexanedione, was observed for all microstructured catalysts containing Brønsted acid sites. The average selectivity toward *p*-xylene for the most promising H–Y catalysts was $51.9 \pm 2.7\%$ at a conversion of $10.7 \pm 2.3\%$ (90% confidence interval).

The observed products of the cycloaddition of dimethylfuran and ethylene are consistent with the proposed furan chemistry of Scheme 2. As shown, catalyzed [4 + 2]-cycloaddition of ethylene to dimethylfuran produces the previously reported bicyclic intermediate, 1,4-dimethyl-7-oxabicyclo[2,2,1]hept-2-ene.^{32,33} Subsequent Brønsted-catalyzed dehydration produces *p*-xylene and water. *p*-Xylene can be further alkylated to produce products such as 1-ethyl-2,5-dimethylbenzene, which are observed in smaller quantities (up to 15% of the converted dimethylfuran is converted to these alkylated products). The formation of water in the dehydration step leads to the hydrolysis of dimethylfuran, which produces the ring-opened product, 2,5-hexanedione. This diketone product can further polymerize to form dimers and larger (uncharacterized) oligomers. Isomerization of *p*-xylene or conversion to toluene

Scheme 2. Schematic of Dimethylfuran Conversion to *p*-Xylene

was not observed, as predicted by equilibrium distributions of xylenes³⁴ (Supporting Information Figure S9).

A two-step reaction through a bicyclic intermediate is consistent with the measured reaction rates and turnover frequencies based on Brønsted acid sites (H-TOF), as shown in Table 1. Although low activity is observed for siliceous

Table 1. Characterization of Considered Catalysts

catalyst	Si/Al ratio	Brønsted acid sites ^a (mmol/g)	total acid sites ^b (mmol/g)	surface area (m ² /g)	H-TOF (s ⁻¹ /10 ³)
H–Y (CBV600)	2.6 ^c	0.36	0.99	660 ^c	0.59
H–Y (CBV760)	30 ^c	0.27	0.64	720 ^c	0.72
H–Y (CBV780)	40 ^c	0.12	0.25	780 ^c	1.70
H-BEA (CP814C)	19 ^c	0.56	1.21	710 ^c	0.24
H-ZSM-5 (CBV3024E)	15 ^c	0.71	1.1	405 ^c	0.19
H-silica–alumina (amorphous)	5 ^d	0.34 ^d	0.43 ^d	585 ^d	
siliceous BEA	NA	NA	NA	475 ^e	NA
silicalite -1	NA	NA	NA	346 ^e	NA
mullite (crystalline)	0.27 ^c	NA	NA	0.24 ^c	NA

^aObtained using isopropylamine-TGA TPD. ^bObtained using ammonia-TPD. ^cProvided by manufacturer. ^dWeingarten et al. ^eObtained using BET equation within $0.05 < P/P_0 < 0.3$

materials and high activity is observed for Brønsted acid-containing materials, it is also apparent that Brønsted acid-catalyzed reactions are not rate-determining in the formation of *p*-xylene. H–Y catalysts with significantly different Brønsted acid site densities (Si/Al = 2.6 and Si/Al = 40) exhibit the same catalytic reaction rate (Figure 1), whereas the H-TOFs for these two materials are very different ($5.9 \times 10^{-4} \text{ s}^{-1}$ and $1.7 \times 10^{-3} \text{ s}^{-1}$ for Si/Al of 2.6 and 40, respectively). There exists no relationship between catalyst activity and Brønsted site density, which indicates that the rate-determining step is the cycloaddition to produce the bicyclic intermediate. Statistically different activities are observed only in zeolites with different microstructures; the cage structure of H–Y zeolite is more active than the channel structure of H-ZSM5 and H-Beta. Consistent with previous literature, the Diels–Alder reaction examined here is enhanced by confinement within pores.^{35–37} This is supported by the low selectivity to *p*-xylene of H-silica–alumina, an amorphous catalyst with no micropore structure but Brønsted site density comparable to the zeolite catalysts.³⁸

The need for a Brønsted site that catalyzes the dehydration step is supported by the computed free energy barriers in Figure 2. The formation of a bicyclic intermediate is not

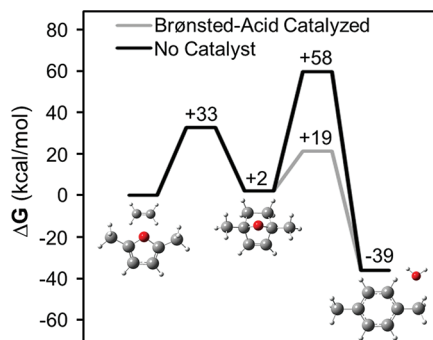


Figure 2. Computed free energy barriers of dimethylfuran cycloaddition with ethylene and dehydration to *p*-xylene at 300 °C. The black line depicts the free energy profile for the uncatalyzed conversion of DMF to *p*-xylene via Diels–Alder cycloaddition and subsequent dehydration in the gas phase. The gray line shows the free energy profile for Brønsted acid-catalyzed dehydration. For the dehydration reaction, only the highest energy barrier is shown.

favorable thermodynamically ($\Delta G_{\text{rxn}} = 2.28$ kcal/mol) at 300 °C, but the product, *p*-xylene, is overwhelming favorable ($\Delta G_{\text{rxn}} = -38.56$ kcal/mol), in accordance with long-time experiments (>24 h), which achieve conversion exceeding $X_{\text{DMF}} = 90\%$; all energies refer to the interacting reactant complex. The kinetic barrier for cycloaddition to produce the bicyclic intermediate is 32.89 kcal/mol, whereas the noncatalyzed dehydration barrier is quite large (57.6 kcal/mol) and qualitatively consistent with low reaction rates of siliceous materials. However, the introduction of Brønsted acid sites significantly lowers the dehydration barrier to 19.13 kcal/mol, thereby making the first step (cycloaddition) rate-determining. This finding is in agreement with the initial catalytic rate experiments (Figure 1) and underscores the necessity of a Brønsted acid catalyst to promote dehydration and ultimately make cycloaddition rate-determining.

The optimum catalyst (H–Y) was investigated at high conversion ($X_{\text{DMF}} > 90\%$) to demonstrate the potential of achieving high yield in the considered catalytic system. As shown in Figure 3, the competitive rates of *p*-xylene formation and ring-opening/polymerization with H–Y vary with temperature, with the best performance occurring at 300 °C. Few uncharacterized oligomers are observed as the experimental carbon balances close at $90 \pm 5\%$ for the H–Y catalyst (Si/Al = 30) at high conversion for all temperatures. An increase in temperature from 200 to 300 °C reduces the selectivity to 2,5-hexanedione and dimers/oligomers such that selectivity to *p*-xylene is $51 \pm 7\%$ for a conversion of $95 \pm 4\%$. The benefit of minimizing the hydrolysis of dimethylfuran was further examined by introducing an aliphatic solvent, *n*-heptane, as shown in Figure 3. By reacting 25 vol % dimethylfuran in *n*-heptane at high conversion ($X_{\text{DMF}} = 95\%$) with H–Y zeolite (Si/Al = 30), the formation of 2,5-hexanedione was reduced to only $2.7 \pm 3.7\%$, and the formation of oligomers was almost negligible, thus achieving a selectivity to *p*-xylene of $75.7 \pm 1.5\%$.

In summary, we have demonstrated that good selectivity ($\sim 75\%$) to *p*-xylene can be achieved at both low (5–10%) and high ($\sim 95\%$) conversion with H–Y zeolite, with the most

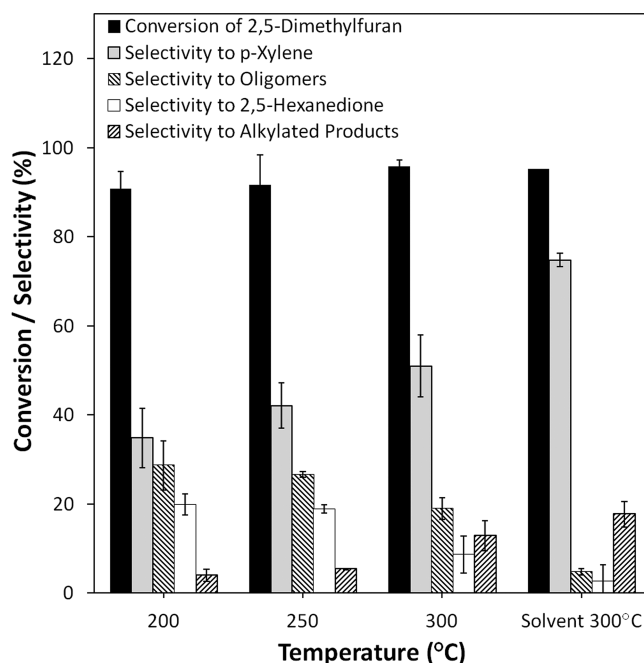


Figure 3. Demonstration of dimethylfuran cycloaddition at high conversion. Increase in reaction temperature from 200 to 300 °C with H–Y zeolite Si/Al = 30 and 900 psig C_2H_4 with pure dimethylfuran exhibits increasing selectivity to *p*-xylene for high conversion of dimethylfuran, $X_{\text{DMF}} > 90\%$. Yield of *p*-xylene further increases by the addition of *n*-heptane solvent (25 vol % DMF/75 vol % *n*-heptane) at 300 °C.

favorable catalysts containing Brønsted acid sites in microporous materials. *p*-Xylene formation competes with ring-opening hydrolysis and polymerization; the latter can be significantly reduced by operating at 300 °C and introducing an aliphatic solvent. The rate of *p*-xylene formation is controlled by the initial cycloaddition step, provided the second dehydration step is Brønsted acid-catalyzed. This catalytic system introduces a new chemical pathway to convert biomass-derived furans to high-value aromatic feedstocks.

■ ASSOCIATED CONTENT

📄 Supporting Information

Details about the catalyst preparation, characterization methods, and reaction procedures. This material is available free of charge via the Internet at <http://pubs.acs.org>.

■ AUTHOR INFORMATION

Corresponding Author

*E-mail: dauenhauer@ecs.umass.edu.

Notes

The authors declare no competing financial interest.

■ ACKNOWLEDGMENTS

This material is supported as part of the Catalysis Center for Energy Innovation, an Energy Frontier Research Center funded by the U.S. Department of Energy, Office of Science, Office of Basic Energy Sciences under Award Number DE-SC0001004.

■ REFERENCES

- (1) Climent, M. J.; Corma, A.; Iborra, S. *Green Chem.* **2011**, *13*, 520–540.

- (2) Ragauskas, A. J.; Williams, C. K.; Davison, B. H.; Britovsek, G.; Cairney, J.; Eckert, C. A.; Frederick, W. J.; Hallett, J. P.; Leak, D. J.; Liotta, C. L.; Mielenz, J. R.; Murphy, R.; Templer, R.; Tschaplinski, T. *Science* **2006**, *311*, 484–489.
- (3) Vlachos, D. G.; Chen, J. G.; Gorte, R. J.; Huber, G. W.; Tsapatsis, M. *Catal. Lett.* **2010**, *140*, 77–84.
- (4) Partenheimer, W. *Catal. Today* **1995**, *23*, 69–158.
- (5) Sheehan, R. J. In *Ullmann's Encyclopedia of Industrial Chemistry*; Wiley-VCH Verlag GmbH & Co. KGaA: Weinheim, 2011; pp 17–28.
- (6) Tsai, T.-C.; Liu, S.-B.; Wang, I. *Appl. Catal., A* **1999**, *181*, 355–398.
- (7) Fong, Y. Y.; Abdullah, A. Z.; Ahmad, A. L.; Bhatia, S. *Chem. Eng. J.* **2008**, *139*, 172–193.
- (8) Ferraro, J. M.; Osman, R. M.; Ou, J. D.-Y.; Cox, G. I.; Lattner, J. R.; Clem, K. R. Process for production of paraxylene, US Patent 6,376,733, April 23, 2002.
- (9) Schmidt, L. D.; Dauenhauer, P. J. *Nature* **2007**, *447*, 914–915.
- (10) Atsumi, S.; Hanai, T.; Liao, J. C. *Nature* **2008**, *451*, 86–89.
- (11) Connor, M. R.; Liao, J. C. *Curr. Opin. Biotechnol.* **2009**, *20*, 307–315.
- (12) Peters, M. W.; Taylor, J. D.; Jenni, M.; Manzer, L. E.; Henton, D. E. Integrated Process to Selectively Convert Renewable Isobutanol to *p*-Xylene, US Patent 20,110,087,000, April 14 2011.
- (13) Lima, S.; Dias, A. S.; Lin, Z.; Brandão, P.; Ferreira, P.; Pillinger, M.; Rocha, J.; Calvino-Casilda, V.; Valente, A. A. *Appl. Catal., A* **2008**, *339*, 21–27.
- (14) Moliner, M.; Román-Leshkov, Y.; Davis, M. E. *Proc. Natl. Acad. Sci. U.S.A.* **2010**, *107*, 6164–8.
- (15) Román-Leshkov, Y.; Chheda, J. N.; Dumesic, J. A. *Science* **2006**, *312*, 1933–1937.
- (16) Román-Leshkov, Y.; Barrett, C. J.; Liu, Z. Y.; Dumesic, J. A. *Nature* **2007**, *447*, 982–985.
- (17) Brandvold, T. A. Carbohydrate Route to *p*-Xylene and Terephthalic Acid, US Patent 20,100,331,568, December 30, 2010.
- (18) Sauer, J.; Sustmann, R. *Angew. Chem. Int. Ed. Engl.* **1980**, *19*, 779–807.
- (19) Kappe, C. O.; Murphree, S. S.; Padwa, A. *Tetrahedron* **1997**, *53*, 14179–14233.
- (20) Balthazor, T. M.; Gaede, B.; Korte, D. E.; Shieh, H. S. *J. Org. Chem.* **1984**, *49*, 4547–4549.
- (21) Shiramizu, M.; Toste, F. D. *Chemistry (Weinheim an der Bergstrasse, Germany)* **2011**, *17*, 12452–7.
- (22) Fraile, J. J. *Mol. Catal. A: Chem.* **1997**, *123*, 43–47.
- (23) McClure, C. K.; Hansent, K. B. *Tetrahedron Lett.* **1996**, *37*, 2149–2152.
- (24) Bornholdt, K.; Lechert, H. *Catal. Microporous Mater.* **1995**, *94*, 619–626.
- (25) Dessau, R. M. *J. Chem. Soc., Chem. Commun.* **1986**, 1167–1168.
- (26) Reymond, S.; Cossy, J. *Chem. Rev.* **2008**, *108*, 5359–406.
- (27) Mintova, S.; Valtchev, V.; Onfroy, T.; Marichal, C.; Knözinger, H.; Bein, T. *Microporous Mesoporous Mater.* **2006**, *90*, 237–245.
- (28) Larlus, O.; Valtchev, V. P.; Werner, A.; Cedex, M. *Chem. Mater.* **2005**, *17*, 881–886.
- (29) Watanabe, R.; Yokoi, T.; Tatsumi, T. *J. Colloid Interface Sci.* **2011**, *356*, 434–41.
- (30) Biaglow, A. I.; Parrillo, D. J.; Gorte, R. J. *J. Catal.* **1993**, *144*, 193–201.
- (31) Frisch, M. J.; Trucks, G. W.; Schlegel, H. B.; Scuseria, G. E.; Robb, M. A.; Cheeseman, J. R.; Scalmani, G.; Barone, V.; Mennucci, B.; Petersson, G. A.; Nakatsuji, H.; Caricato, M.; Li, X.; Hratchian, H. P.; Izmaylov, A. F.; Bloino, J.; Zheng, G.; Sonnenberg, J. L.; Hada, M.; Ehara, M.; Toyota, K.; Fukuda, R.; Hasegawa, J.; Ishida, M.; Nakajima, T.; Honda, Y.; Kitao, O.; Nakai, H.; Vreven, T.; Montgomery, J. A., Jr.; Peralta, J. E.; Ogliaro, F.; Bearpark, M.; Heyd, J. J.; Brothers, E.; Kudin, K. N.; Staroverov, V. N.; Kobayashi, R.; Normand, J.; Raghavachari, K.; Rendell, A.; Burant, J. C.; Iyengar, S. S.; Tomasi, J.; Cossi, M.; Rega, N.; Millam, N. J.; Klene, M.; Knox, J. E.; Cross, J. B.; Bakken, V.; Adamo, C.; Jaramillo, J.; Gomperts, R.; Stratmann, R. E.; Yazyev, O.; Austin, A. J.; Cammi, R.; Pomelli, C.; Ochterski, J. W.; Martin, R. L.; Morokuma, K.; Zakrzewski, V. G.; Voth, G. A.; Salvador, P.; Dannenberg, J. J.; Dapprich, S.; Daniels, A. D.; Farkas, Ö.; Foresman, J. B.; Ortiz, J. V.; Cioslowski, J.; Fox, D. J. *Gaussian09*; Gaussian, Inc.: Wallingford CT, 2009.
- (32) Schmerling, L. Preparation of Alkyl Substituted Aromatic Compounds, US Patent 2,781,407, Feb. 12, 1957.
- (33) Takanishi, K.; Sone, S. Method for Producing *p*-Xylene, WO/2009/110402, Nov. 9 2009.
- (34) Gendy, T. S. *J. Chem. Technol. Biotechnol.* **1998**, *73*, 109–118.
- (35) Zicovich-Wilson, C. M.; Corma, A.; Viruela, P. *J. Phys. Chem.* **1994**, *98*, 10863–10870.
- (36) Gomez, V. M.; Cantin, A.; Corma, A.; de la Hoz, A. *J. Mol. Catal. A: Chem.* **2005**, *240*, 16–21.
- (37) Mashayekhi, G.; Ghandi, M.; Farzaneh, F.; Shahidzadeh, M.; Najafi, H. M. *J. Mol. Catal. A: Chem.* **2007**, *264*, 220–226.
- (38) Weingarten, R.; Tompsett, G. A.; Conner, W. C.; Huber, G. W. *J. Catal.* **2011**, *279*, 174–182.